UNIVERSIDAD NACIONAL DE COLOMBIA
SEDE MEDELLÍN
FACULTAD DE MINAS

DYNA
http://dyna.medellin.unal.edu.co/

An adaptive controller applied to an anti–lock braking system laboratory

Cuauhtémoc Acosta-Lúa [a], Stefano Di Gennaro [b] & María Eugenia Sánchez-Morales [a]

[a] *Centro Universitario de la Ciénega - Universidad de Guadalajara, Ocotlán, Jalisco, México. cuauhtemoc.acosta@cuci.udg.mx, eugenia.sanchez@cuci.udg.mx*
[b] *Department of Information Engineering, Computer Science and Mathematics; also: Center of Excellence DEWS University of L'Aquila, Coppito, L'Aquila, Italy. stefano.digennaro@univaq.it*

Recibido: July 13th, 2015. Recibido en versión revisada: April 11 th, 2016. Aceptado: June 13th, 2016.

Abstract
Controlling an antilock braking system is difficult due to the existence of nonlinear dynamics and the uncertainty of its characteristics and parameters. To overcome these issues, we propose two controllers. The first controller is designed under the complete knowledge of the parameters hypothesis. Then, an adaptive nonlinear controller is designed using an estimate of the tire–road friction coefficient. This second controller is implemented in an ABS laboratory setup in order to test its performance, and the results show that the adaptive controller ensures the tracking of the desired reference and identifies the unknown parameter.

Keywords: Adaptive Control, Anti–lock braking system, Real–Time Systems, Wheel Slip Control.

Control adaptivo aplicado a un laboratorio de un sistema de frenos antibloqueo

Resumen
El control para un sistema de frenos antibloqueo (ABS) es un problema complejo debido a la existencia de dinámicas no lineales y perturbaciones en algunos parámetros. Para hacer frente a estos problemas, se proponen dos controladores. El primer controlador es diseñado bajo la hipótesis de que se conocen todos los parámetros. Enseguida, se diseña un controlador adaptivo usando una estimación del coeficiente de fricción neumático–carretera. Este segundo controlador es implementado en un laboratorio de ABS para probar la eficacia del mismo, y los resultados muestran que el controlador adaptivo asegura el seguimiento de la referencia deseada e identifica el parámetro desconocido.

Palabras clave: Control Adaptivo; Sistema de Frenos Antibloqueo, Sistemas en Tiempo real, Control de Deslizamiento en las ruedas.

1. Introduction

The Antilock Braking System (ABS) is an electronically controlled system that helps the driver to maintain the control of the vehicle during emergency braking. It achieved this by preventing the wheels from locking–up. This prevents the slippage of the wheels on the surface, adjusting the brake fluid pressure level of each wheel, and helps the driver to keep the control of the vehicle [1]. Increasing the braking efficiency and maintaining the vehicle's maneuverability, the ABS reduces driving instability and decreases the braking distance by adjusting the maximum braking power applied to the brake pad. Modern ABS systems aim to obtain maximum wheel grip on the surface while the vehicle is braking [2] as well as preventing the wheels from locking–up.

Several algorithms have been designed to control ABS systems. These control algorithms can be grouped in two main categories: wheel acceleration and tire slip control. The first category approaches slip control indirectly by controlling the deceleration/acceleration of the wheel through the brake pressure from the actuator. The second control is a direct wheel slip control. This kind of controller

How to cite: Acosta-Lúa, C., Di Gennaro, S. & Sánchez-Morales, M. U. An Adaptive Controller Applied to an Anti–lock Braking System Laboratory DYNA 83 (199) pp. 69-77, 2016

is not easy to design because of the highly nonlinear and uncertain structure of the ABS system.

One of the main issues is that the controller has to operate at an unstable equilibrium point in order to achieve optimal behavior. Small perturbations of the controller input may induce drastic changes in the output. The performance of the ABS system is not always satisfactory due to the high dependency of the system parameters on the road conditions, which may vary over a wide range and in an unexpected manner. All these factors complicate the development of an accurate mathematical model for the ABS system. Therefore, advanced control design techniques are required so that the wheel slip control can cope with uncertainties in the dynamic models.

Different (linear and nonlinear) techniques have been developed to control ABS systems. The design of braking control systems faces important challenges, generally associated with velocity and vehicle parameters estimation. In [3] an extended Kalman filter is used to estimate the friction coefficient with the corresponding simulations in CarSim. Using intelligent control, in [4], a self–learning fuzzy sliding–mode control (SLFSMC) design method was proposed. In [5], a fuzzy model reference learning controller, a genetic model reference adaptive controller, and a general genetic adaptive controller were designed. Another ABS control technique is the hybrid control that was introduced by [6,7]. Moreover, [8] describes the analysis, modeling and simulation of an electric vehicle (EV) focused on developing a test bench to reproduce EV dynamics using de ABS system. In [9], an ABS for an electric vehicle was designed, whereas [10] introduces an electrical ABS actuating in wheel motors.

In this article a mechatronic system, the ABS laboratory setup manufactured by Inteco Ltd, was used to test a proposed nonlinear adaptive controller. This experimental setup represents a quarter car model and consists of two rolling wheels. The lower wheel, made of aluminum, emulates the relative road motion of the car, whereas the upper wheel, made of rigid plastic, is mounted on the balance lever and simulates the wheel of a vehicle. In order to accelerate the lower wheel, a large DC motor is coupled on it. The upper wheel is equipped with a disk–brake system that is driven by a small DC motor where the control input is applied [11]. Encoders on the wheels allow their positions and velocities to be determined. The proposed control ensures that the desired references are tracked, using information available from the ABS sensors, i.e. the angular velocity of the upper and lower wheels. The main achievement of this article is regarding the parameter adaptation of the friction coefficient between the two wheels; this represents the tire–road friction coefficient in a real automobile. This is one of the most important parameters, the estimation of which can be difficult, for example in the case of sudden variations due to changes in road conditions. The adaptation in the controller guarantees the exponential convergence of the estimation to the real parameter value, as well as the exponential tracking of the reference. Finally, the nonlinear adaptive controller has been implemented and validated through real–time simulations on the ABS laboratory setup.

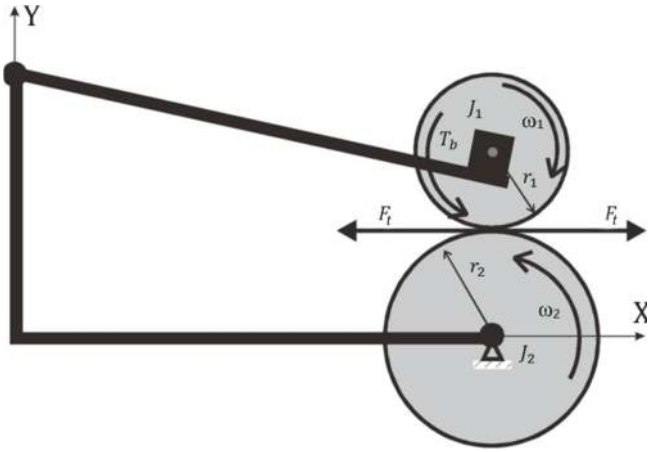

Figure 1. Scheme of the ABS laboratory setup.
Source: Inteco Manual [11].

Earlier works focused on ABS laboratory setups are mainly based on the assumption that all sensors´ information is available for measurement. Some works present linear and nonlinear controllers [12,13], whereas [14] proposes a fuzzy control. In [15] a control strategy based on sliding mode is proposed. Finally, some articles use intelligent control techniques [16,17].

The article is organized as follows: section 2 briefly presents the mathematical model of the experimental setup. In Section 3, the control problem is solved to track a constant reference when the state variables are considered measurable. First, all the parameters are considered known. Then, the friction coefficient between the wheels is considered unknown, and an estimation is proposed. Section 4 shows some real–time results obtained using the ABS laboratory setup. The paper ends with some concluding remarks.

2. Mathematical model of the experimental ABS laboratory setup

In this paper, an ABS laboratory setup manufactured by Inteco Ltd. was considered (see Fig. 1). Although simple, this setup preserves the fundamental characteristics of an actual ABS system in the range of 0–70 km/h [11].

2.1. Mathematical model of the ABS laboratory setup

The mathematical model of the ABS laboratory setup is derived under the assumptions of negligible lateral and vertical motions, and a rolling resistance force negligible with respect to braking (see Fig.2). The braking torque $\boldsymbol{T_b}$ and the bearing friction torque $\boldsymbol{M_{10}}$ act on the upper wheel. The bearing friction torque $\boldsymbol{M_{20}}$ acts on the lower wheel. The tractive force $\boldsymbol{F_t}$ acts on both wheels.

The dynamic equations of the ABS laboratory setup are

$$\begin{aligned}\dot{\omega}_1 &= \frac{r_1}{J_1}F_t s(\omega) - \frac{1}{J_1}(d_1\omega_1 + M_{10} + T_b)s_1(\omega_1)\\ \dot{\omega}_2 &= -\frac{r_2}{J_2}F_t s(\omega) - \frac{1}{J_2}(d_2\omega_2 + M_{20})s_2(\omega_2)\end{aligned} \quad (1)$$

where $\boldsymbol{\omega_1}$, $\boldsymbol{\omega_2}$ are the angular velocities of the upper and lower wheels respectively, the inertia moments of which are $\boldsymbol{J_1}, \boldsymbol{J_2}$ and the radii of which are $\boldsymbol{r_1}, \boldsymbol{r_2}$. Furthermore, $\boldsymbol{d_1}$, $\boldsymbol{d_2}$ are the viscous friction coefficients of the upper and lower wheel, $\boldsymbol{M_{10}}$, $\boldsymbol{M_{20}}$ are the static frictions of the upper and lower wheel, respectively, $\boldsymbol{T_b}$ is the braking torque, and $\boldsymbol{F_t}$ is the traction force between the wheels. The nominal parameters are given in Table 1. Finally, $\boldsymbol{s(\omega)}$, $\boldsymbol{s_1(\omega)}$ and $\boldsymbol{s_2(\omega)}$ are auxiliary variables used to determinate if the vehicle is in traction mode or in braking mode

$$s(\omega) = \text{sign}(r_2\omega_2 - r_1\omega_1) \quad s_1(\omega_1) = \text{sign}(\omega_1), \quad s_2(\omega_2) = \text{sign}(\omega_2) \tag{2}$$

with

$$\text{sign}(\omega) = \begin{cases} 1 & \text{if } \omega > 0 \\ 0 & \text{if } \omega = 0 \\ -1 & \text{if } \omega < 0. \end{cases} \tag{3}$$

Here $v_\omega = r_1\omega_1$ represents the vehicle wheel velocity, whereas $v_x = r_2\omega_2$ represents the vehicle velocity. The tractive force F_t is generated on contact between the upper and the lower wheel. Various models are available in the literature to model the tire behavior [18]. Without loss of generality, since the same approach can be used with different tire models, in this work the simplified Pacejka's "magic formula" [16]

$$F_t = \mu D_t \sin(C_t \arctan(B_t\lambda)) \tag{4}$$

has been used to describe the tractive force, where

$$\lambda = \frac{r_2\omega_2 - r_1\omega_1}{r_2\omega_2} \tag{5}$$

is the wheel slip, i.e. the relative difference of the wheel velocities. This formula approximates the response curve of the braking process based on experimental data. It is widely used, and makes it possible to work with a wider range of values, both in the linear and in the nonlinear region of the tire characteristic.

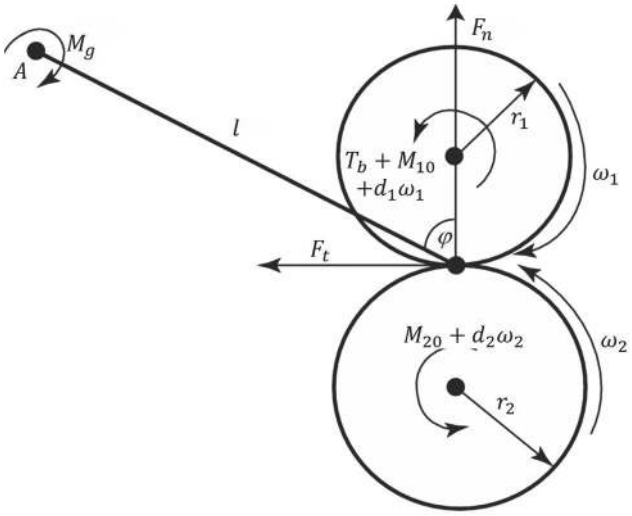

Figure 2. Forces and torques acting on the ABS laboratory setup.
Source: Inteco Manual [11].

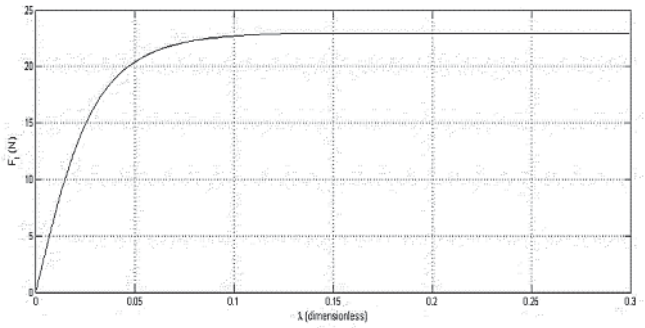

Figure 3. Typical characteristic of the tractive force F_t as function of the wheel slip angle λ.
Source: The authors.

The expression (4) of the tractive force F_t depends on positive experimental coefficients given by the stiffness factor B_t; the shape factor C_t; and the peak value D_t, which are determined to match the experimental data. Moreover, $\mu \in [0,1]$ is the friction coefficient between the upper and lower wheel. Fig. 3 shows the characteristic of the tractive force calculated with (4), as a function of the wheel slip (5).

The braking torque, T_b, is modeled with a first–order equation [11], given by

$$\dot{T}_b = -c_{31}T_b + c_{31}b(u) \tag{6}$$

where c_{31} is a positive constant, and $b(u)$ describes the relation between the control input applied to the DC motor, which drives the action of brake pads, and the control input $\mu \in [0,1]$, which generates the braking torque T_b. This relation can be approximated by

$$b(u) = \begin{cases} b_1u + b_2 & \text{if } u \geq u_0 \\ 0 & \text{if } u < u_0 \end{cases} \tag{7}$$

where u_0 is the operating threshold of the brake driving system. According to the mathematical model, equation (6) is similar to the brake pedal in an automobile [17,20–21].

Under normal operational conditions, the wheel velocity $v_\omega = r_1\omega_1$ matches the forward velocity $v_x = r_2\omega_2$. When the brake is applied, braking forces are generated at the wheel interface and v_ω tends to be lower than v_x (but always positive), this a slippage occurs. During the braking process, the wheel slip λ is positive, as well as ω_1, ω_2. Hence,

$$s(\omega) = \text{sign}(r_2\omega_2 - r_1\omega_1) = 1 \quad s_1(\omega_1) = \text{sign}(\omega_1) = 1, \quad s_2(\omega_2) = \text{sign}(\omega_2) = 1 \tag{8}$$

and equations (1) become

$$\dot{\omega}_1 = \frac{r_1}{J_1}F_t - \frac{1}{J_1}(d_1\omega_1 + M_{10} + T_b) \quad \dot{\omega}_2 = -\frac{r_2}{J_2}F_t - \frac{1}{J_2}(d_2\omega_2 + M_{20}). \tag{9}$$

2.2. Longitudinal vehicle force

The tractive force F_t given in (4) can be rewritten as

$$F_t = \theta\varphi(\lambda),\ \ \varphi(\lambda) = \sin(C_t \arctan(B_t\lambda)) \tag{10}$$

where $\theta = \mu D_t$ is the product of the road–tire friction coefficient with the tire stiffness coefficient D_t, and where $\varphi(\lambda)$ is the normalized tire characteristics. This latter usually increases linearly with the wheel slip λ up to a maximum value and then decreases, reaching an asymptotic value for high wheel slip angles, as shown in Fig. 3. The function $\varphi(\lambda)$ is symmetric with respect to the origin. Hence, $\varphi(\lambda)$ reaches a minimum for negative values of λ and then increases to an asymptotic value for high negative wheel slip angles.

In real automobiles the friction coefficient is a parameter that may vary considerably according to the road and tire conditions. Also, the parameter D_t depends on the tire conditions. Considering (10), equations (1) can be rewritten in the following form:

$$\begin{aligned}\dot{\omega}_1 &= \frac{r_1}{J_1}\theta\varphi(\lambda) - \frac{1}{J_1}(d_1\omega_1 + M_{10} + T_b)\\ \dot{\omega}_2 &= -\frac{r_2}{J_2}\theta\varphi(\lambda) - \frac{1}{J_2}(d_2\omega_2 + M_{20}).\end{aligned} \tag{11}$$

In the following section it is assumed, that $v_x \geq 0$. The output to be controlled is the wheel slip λ and the control aim is to design a controller such that λ globally tracks a constant reference λ_{ref} in the presence of parameter uncertainties. The primary function of the controller is to prevent the lock–up of the wheel during an emergency brake. Ideally, it is desired that the ABS maintains the wheel slip at the peak of the maximum longitudinal (tractive) force $F_t(\lambda)$. Hence, it is considered to be a constant reference λ_{ref} [19].

3. Design of an Adaptive Nonlinear Controller

In the following section it is assumed that only the parameter nominal values μ_0, $D_{t,0}$ are known. Therefore, θ is unknown, with a nominal value $\theta_0 = \mu_0 D_{t,0}$. In this section a nonlinear dynamic controller is designed to force the error

$$e_\lambda = \lambda - \lambda_{\text{ref}} \tag{12}$$

to zero in the presence of variations of θ. The control law needs to generate a control reference. Hence, instead of considering the wheel slip as the controlled variable, the auxiliary slip velocity $v_s = v_x - v_\omega = \lambda v_x$ will be used. The slip velocity reference is given by $v_{s,\text{ref}} = \lambda_{\text{ref}} v_x$. Hence, the slip velocity error is defined as

$$e_v = v_s - v_{s,\text{ref}} = e_\lambda v_x = (1-\lambda_{\text{ref}})v_x - v_\omega. \tag{13}$$

Since $v_x \neq 0$, the control problem is equivalent to force e_v to zero asymptotically. The dynamics of the slip velocity error are

$$\begin{aligned}\dot{e}_v &= (1-\lambda_{\text{ref}})\dot{v}_x - \dot{v}_\omega = (1-\lambda_{\text{ref}})r_2\dot{\omega}_2 - r_1\dot{\omega}_1\\ &= -k(\lambda_{\text{ref}})\theta\varphi(\lambda) + \frac{r_1}{J_1}(d_1\omega_1 + M_{10} + T_b)\\ &\quad -(1-\lambda_{\text{ref}})\frac{r_2}{J_2}(d_2\omega_2 + M_{20})\end{aligned} \tag{14}$$

where

$$k(\lambda_{\text{ref}}) = \frac{r_1^2}{J_1} + (1-\lambda_{\text{ref}})\frac{r_2^2}{J_2}. \tag{15}$$

Considering a constant slip reference λ_{ref}, if the parameter θ_0 is known and $\omega_1, \omega_2, M_{10}, M_{20}$ are measurable, the controller

$$\begin{aligned}\dot{I}_{ev} &= e_v\\ T_b &= \frac{J_1}{r_1}\xi_1\\ \xi_1 &= -k_{s0}I_{ev} - k_{s1}e_v + k(\lambda_{\text{ref}})\theta_0\varphi(\lambda)\\ &\quad -\frac{r_1}{J_1}(d_1\omega_1 + M_{10})\\ &\quad +(1-\lambda_{\text{ref}})\frac{r_2}{J_2}(d_2\omega_2 + M_{20})\end{aligned} \tag{16}$$

with $k_{s0}, k_{s1} > 0$, ensures that the tracking error (13) and its derivative globally and exponentially converge to zero.

In fact, $\dot{e}_v = -k_{s0}I_{ev} - k_{s1}e_v$ is easily reached and, $\ddot{e}_v + k_{s0}e_v + k_{s1}\dot{e}_v = 0$ is easily derived. Hence, e_v, $\dot{e}_v$ tend globally exponentially to zero, as well as the error e_λ in (12). Hence λ tends to λ_{ref} globally and exponentially.

Let us now consider the case in which the friction coefficient θ between the two wheels is unknown.

Theorem 3.1 Consider a constant slip reference λ_{ref}. If the disturbances M_{10}, M_{20} are known and constant, ω_1, ω_2 are measurable, and the parameter θ is unknown, the dynamic controller

$$\begin{aligned}\dot{I}_{ev} &= e_v\\ \dot{\hat{\omega}}_1 &= \frac{r_1}{J_1}\hat{\theta}\varphi(\lambda) - \frac{1}{J_1}(d_1\omega_1 + M_{10} + T_b)\\ \dot{\zeta} &= -\gamma k(\lambda_{\text{ref}})\varphi(\lambda)B^T P\begin{pmatrix} I_{e_v}\\ e_v\end{pmatrix}\\ T_b &= \frac{J_1}{r_1}\hat{\xi}_1\end{aligned} \tag{17}$$

with

$$\begin{aligned}\hat{\theta} &= \zeta - \gamma k_{a1}\frac{J_1}{r_1}(\omega_1 - \hat{\omega}_1)\\ \hat{\xi}_1 &= -k_{s0}I_{ev} - k_{s1}e_v + k(\lambda_{\text{ref}})\hat{\theta}\varphi(\lambda)\\ &\quad -\frac{r_1}{J_1}(d_1\omega_1 + M_{10}) + (1-\lambda_{\text{ref}})\frac{r_2}{J_2}(d_2\omega_2 + M_{20})\end{aligned} \tag{18}$$

and with $k(\lambda_{\text{ref}})$ as (15) and $k_{s0}, k_{s1}, k_{a1} > 0$, ensures

that the tracking error (13) and the estimation error $\tilde{\theta} = \theta - \hat{\theta}$ globally exponentially tend to zero along their derivatives.

Proof 1. The dynamics of the error (14) rewrite

$$\dot{e}_v = -k(\lambda_{\text{ref}})\theta\varphi(\lambda) + \frac{r_1}{J_1}(d_1\omega_1 + M_{10}) + \frac{r_1}{J_1}T_b$$
$$-(1-\lambda_{\text{ref}})\frac{r_2}{J_2}(d_2\omega_2 + M_{20}) - k_{s0}I_{ev} + k_{s0}I_{ev}$$
$$-k_{s1}e_v + k_{s1}e_v + k(\lambda_{\text{ref}})\hat{\theta}\varphi(\lambda) - k(\lambda_{\text{ref}})\hat{\theta}\varphi(\lambda).$$

Hence, using (17), (18), the error dynamics are

$$\begin{pmatrix}\dot{I}_{ev}\\ \dot{e}_v\end{pmatrix} = A\begin{pmatrix}I_{ev}\\ e_v\end{pmatrix} + B\left(-k(\lambda_{ref})\varphi(\lambda)\right)\tilde{\theta}$$

with the matrices

$$A = \begin{pmatrix}0 & 1\\ -k_{s0} & -k_{s1}\end{pmatrix}, \quad B = \begin{pmatrix}0\\ 1\end{pmatrix}.$$

Let us consider the following Lyapunov candidate

$$V = V_e + V_\theta$$

with

$$V_e = \frac{1}{2}\begin{pmatrix}I_{ev}\\ e_v\end{pmatrix}^T P\begin{pmatrix}I_{ev}\\ e_v\end{pmatrix}, \quad V_\theta = \frac{1}{2\gamma}\tilde{\theta}^2$$

and where $P = P^T > 0$. Deriving along the trajectories of the system

$$\dot{V}_e = -\left\|\begin{matrix}I_{ev}\\ e_v\end{matrix}\right\|_Q^{\cdot 2} + \tilde{\theta}B^TP\left\|\begin{matrix}I_{ev}\\ e_v\end{matrix}\right\|\left(-k(\lambda_{ref})\varphi(\lambda)\right)$$

And

$$\dot{V}_\theta = -\frac{1}{\gamma}\tilde{\theta}\dot{\hat{\theta}}$$

so that one obtains

$$\dot{V} = -\left\|\begin{matrix}I_{ev}\\ e_v\end{matrix}\right\|_Q^2 + \tilde{\theta}\left(-\dot{k}(\lambda_{ref})\varphi(\lambda)\right)B^TP\left\|\begin{matrix}I_{ev}\\ e_v\end{matrix}\right\| + \frac{1}{\gamma}\tilde{\theta}\dot{\tilde{\theta}}$$

with $Q = Q^T > 0$ fixed, and P solution of the Lyapunov equation $PA + A^TP = -2Q$. Since $\dot{\tilde{\theta}} = \dot{\theta} - \dot{\hat{\theta}} = -\dot{\hat{\theta}}$, and considering the dynamics of $\dot{\omega}_1$, one obtains

$$\dot{\hat{\theta}} = -\dot{\zeta} + \gamma k_{a1}\frac{J_1}{r_1}(\dot{\omega}_1 - \dot{\hat{\omega}}_1).$$

Therefore, one obtains

$$\dot{V} = -\left\|\begin{matrix}I_{ev}\\ e_v\end{matrix}\right\|_Q^2 - k_{a1}\varphi(\lambda)\tilde{\theta}^2 \le -\lambda_{\min}^Q\left\|\begin{matrix}I_{ev}\\ e_v\end{matrix}\right\|^2 - k_{a1}\varphi_{\max}\tilde{\theta}^2$$

since $0 < \varphi(\lambda) \le \varphi_{\max}$, and where $\lambda_{\min}^Q$ is the minimum eigenvalue of Q. Therefore, I_{ev}, e_v, and $\tilde{\theta}$ tend to zero globally and exponentially. Hence, v_s tends to $v_{s,\text{ref}}$ globally and exponentially. Since the adaptive controller (17) ensures that $v_s \to v_{s,\text{ref}}$ globally an exponentially, one concludes that also λ tends to λ_{ref} globally and exponentially.

Theorem 3.2 Assume that *the parameter θ remains bounded, varying with bounded derivative $\|\dot{\theta}\| \le \Delta$, for a certain $\Delta > 0$. Hence, the controller of Theorem 3.2 ensures global practical exponential stability of the tracking error (13) and of the estimation error dynamic $\tilde{\theta} = \theta - \hat{\theta}$ to a ball of the origin of arbitrary radius $\varepsilon > 0$.*

Proof 2. Following the proof of Theorem 1, one obtains

$$\dot{V} \le -\lambda_{\min}^Q\left(\left\|\begin{matrix}I_{ev}\\ e_v\end{matrix}\right\|^2 + \|\tilde{\theta}\|^2\right) + \tilde{\theta}^T\dot{\theta}$$
$$\dot{V} \le -\lambda_{\min}^Q\left(\left\|\begin{matrix}I_{ev}\\ e_v\end{matrix}\right\|^2 + \|\tilde{\theta}\|^2\right)\|\tilde{\theta}\|\Delta$$
$$\le -\lambda_{\min}^Q\left(\left\|\begin{matrix}I_{ev}\\ e_v\end{matrix}\right\|^2 + \|\tilde{\theta}\|^2\right) + \sqrt{\left\|\begin{matrix}I_{ev}\\ e_v\end{matrix}\right\|^2 + \|\tilde{\theta}\|^2}\Delta$$

for $\|\dot{\theta}\| \le \Delta$. Since

$$\lambda_1\left(\left\|\begin{matrix}I_{ev}\\ e_v\end{matrix}\right\|^2 + \|\tilde{\theta}\|^2\right) \le V \le \lambda_2\left(\left\|\begin{matrix}I_{ev}\\ e_v\end{matrix}\right\|^2 + \|\tilde{\theta}\|^2\right)$$

with $\lambda_1 = \min\{\lambda_{\min}^P, \gamma\}$, $\lambda_2 = \max\{\lambda_{\max}^P, \gamma\}$, then

$$\dot{V} \le -\frac{\lambda_{\min}^Q}{\lambda_2}V + \frac{1}{\sqrt{\lambda_1}}\sqrt{V}$$

or, setting $V = W^2$,

$$W \le -\dot{a_1}W + a_0, \quad a_1 = \frac{\lambda_{min}^Q}{2\lambda_2}, \qquad a_0 = \frac{1}{2\sqrt{\lambda_1}}$$

so that

$$\sqrt{\lambda_1}\sqrt{\left\|\begin{matrix}I_{ev}\\ e_v\end{matrix}\right\|^2 + \|\tilde{\theta}\|^2} \le \sqrt{V} = W(t)$$
$$\le e^{-a_1t}\left(W(0) - \frac{a_0}{a_1}\right) + \frac{a_0}{a_1} \to \frac{a_0}{a_1}.$$

Setting $\frac{a_0}{\sqrt{\lambda_1}a_1} \le \varepsilon$, i.e.

$$\lambda_{\min}^Q \ge \frac{\lambda_2}{\varepsilon\sqrt{\lambda_1}}$$

one ensures that

$$\sqrt{\left\|\begin{matrix} I_{ev} \\ e_v \end{matrix}\right\|^2 + \|\tilde{\theta}\|^2} \leq \varepsilon$$

i.e. global practical exponential stability to an arbitrary ball of the origin.

4. Experimental Results

In order to compare the performance of the proposed controller with another that is available in literature, we present a comparison with a sliding–mode controller that was proposed in [16], which uses an estimation $\hat{\theta}$ of θ. The sliding–mode technique is a very efficient control technique because of its properties concerning order reduction and low sensibility to disturbances and parameter variation [22]. This is important in the control of nonlinear systems such as the ABS. The high–frequency nature of the SMC signal is its main drawback because the control can excite non–modeled system dynamics and wear out mechanical parts.

Experimental tests on the ABS laboratory setup (see Fig. 4) have been conducted to evaluate the braking performance of the proposed controller (17) using the data in Table 1. These tests represent maneuvers in a straight line. The initial conditions were $\omega_1(0) = \omega_2(0) =$1625 RPM (170 rad/s) and $\zeta(0) = 0$.

When the maximal velocity of the upper wheel is detected, the system disables the DC motor coupled to the lower wheel, and the braking process begins. It is worthwhile noting that this work considers $\mu_0 = 1$, but in terms of the real system its variability can be taken into account, varying μ_0 in the interval of interest.

Figure 4. The ABS laboratory setup [11].
Source: Inteco Manual [11].

Table 1.
The ABS laboratory setup´s coefficients and system variables of the.

Variable	Description	Value
ω_1	Angular velocity of the upper wheel	rad/s
ω_2	Angular velocity of the lower wheel	rad/s
T_b	Braking torque	Nm
r_1	Radius of the upper wheel	0.0995 m
r_2	Radius of the lower wheel	0.0990 m
J_1	Upper wheel inertia moment	$7.54\text{x}10^{-3}$ kg m^2
J_2	Lower wheel inertia moment	$25.60\text{x}10^{-3}$ kg m^2
d_1	Upper wheel viscous friction coefficient	$118.74\text{x}10^{-6}$ kg m^2/s
d_2	Lower wheel viscous friction coefficient	$214.68\text{x}10^{-6}$ kg m^2/s
μ_0	Friction coefficient between wheels	1
M_{10}	Static friction of the upper wheel	0.0032 N m
M_{20}	Static friction of the lower wheel	0.0925 N m
b_1	Constant	15.24
b_2	Constant	-6.21
c_{31}	Constant	20.37 s^{-1}
u_0	Constant	0.415
u	Control input	
D_t	Peak value	23
C_t	Peak value	1.68
B_t	Stiffness factor	28
γ	Adaptive Gain	21
k_{s0}	Controller Gain	19
k_{s1}	Controller gain	32

Source: Inteco Manual [11].

The results are summarized in Figs. 5–10, in which it can be seen that the proposed controller (17) ensures better performances with respect to the sliding–mode controller [15]. It is important to emphasize that after the braking phase, between 6.2 and 7.4 s, which correspond to the maximum braking efficiency, the performance is no longer relevant since the longitudinal velocity is low, and the setup is no longer working in the appropriate range of velocities. In fact, λ will grow when the longitudinal velocity tends to zero. Figs. 5 and 6 show that both controllers maintain deceleration in both velocities. The difference can be found in the time the controllers require to complete the braking process. The proposed controller (17) manages to stop a few tenths of a second before the sliding–mode controller. Furthermore, as shown in Fig. 7, the proposed controller (17) reaches faster the reference $\lambda_{\text{ref}} = 0.15$, and keeps the estimated slip closer to the reference.

Another positive effect of the proposed controller is shown in Fig. 8, in which the absence of chattering, typical of the sliding–mode control can be seen. This ensures better wear resistance, less noise, and an increased passenger comfort with lower jerk effects. Fig. 9 shows, for both controllers, the estimate $\hat{\theta}$ of the real parameter. At the end of the braking process, the estimate is not reliable since $\hat{\theta}$ depends on the slip velocity λ, which is not properly controlled at the end of the braking process. This has already been commented upon.

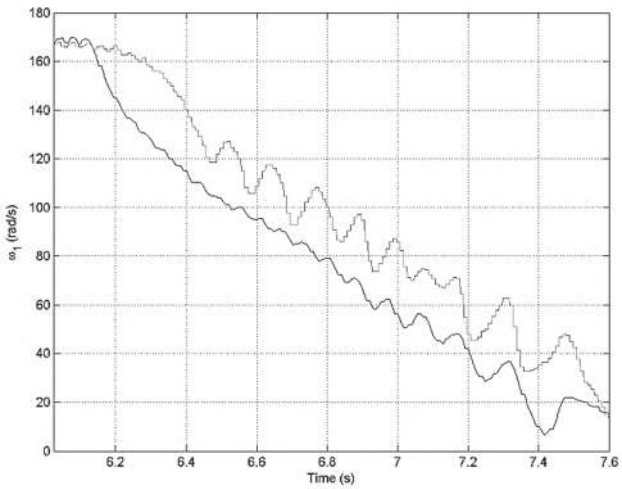

Figure 5. Upper wheel angular velocity ω_1: Proposed controller (17) (black) and sliding–mode control (gray).
Source: The authors.

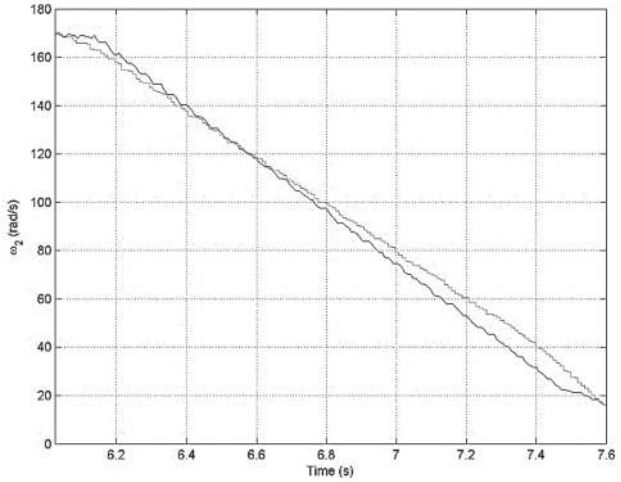

Figure 6. Lower wheel angular velocity ω_2: Proposed controller (17) (black) and sliding–mode control (gray).
Source: The authors.

As a final indication of the better performance of the proposed controller, Fig. 10 shows that the proposed controller (17) accomplishes the braking process in approximately 6.7% less time and distance in comparison with the sliding–mode controller.

4. Conclusions

This article presents an adaptive controller for an ABS laboratory setup. The proposed controller allows the friction coefficient between the two wheels to be identified. It is assumed that the bearing friction torques are known. The adaptive controller is designed to ensure the exponential stability of the system. In addition, the dynamic controller ensures the desired tracking of the wheel slip, and is implemented in real–time.

A series of experiments have been performed on the ABS Laboratory setup to show the performance of the proposed

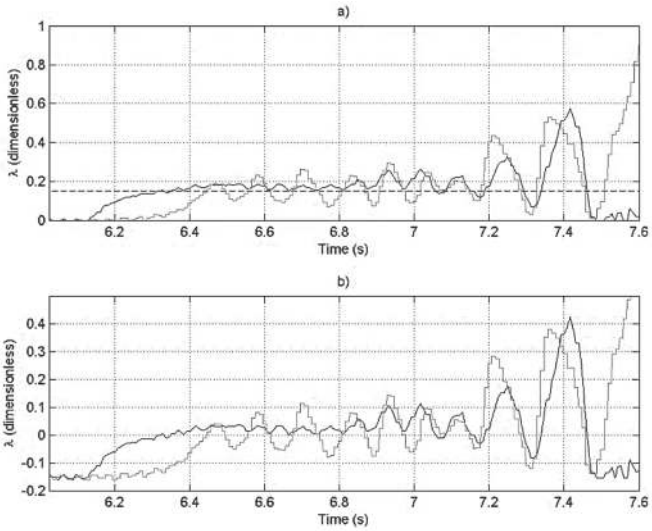

Figure 7. a) Wheel slip λ Proposed controller (17) (black), sliding–mode control (gray) and wheel slip reference $\hat{\lambda}_{\text{ref}}$ (dashed); b) Tracking error $\lambda - \hat{\lambda}_{\text{ref}}$: Proposed controller (17) (black), sliding–mode control (gray).
Source: The authors.

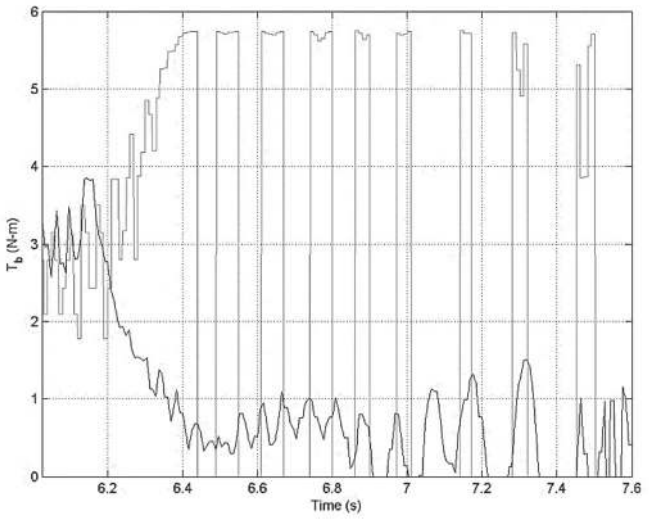

Figure 8. Input control applied to system T_b [N m vs s]: Proposed controller (17) (black); sliding–mode control (gray).
Source: The authors.

adaptive controller. The experimental results also show the performance of this dynamic controller in comparison with a sliding–mode control that was proposed in the literature.

The sliding–mode controller suffers from chattering, which is absent in the proposed controller and thus shows better behavior. Moreover, the proposed controller achieves shorter braking distances in shorter times, hence increasing safety. Finally, thanks to a smoother signal to the actuator with respect to the sliding–mode control, the proposed controller ensures longer durability of the pads, less noise, and an increased passenger comfort with lower jerk effects.

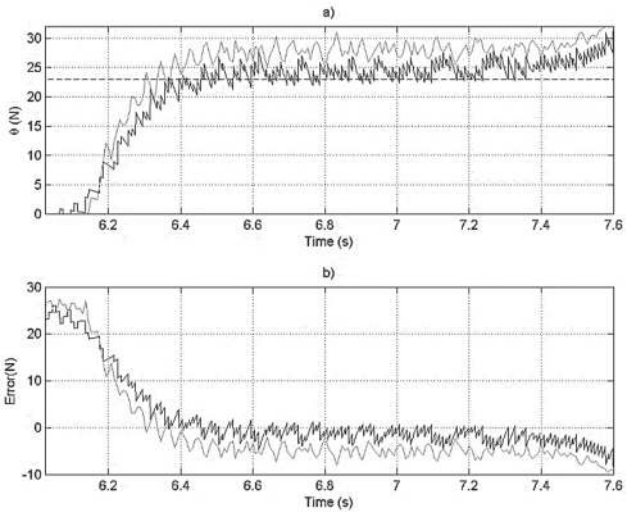

Figure 9. a) ABS laboratory parameter: Real θ (dashed) and estimated $\hat{\theta}$: Proposed controller (17) (black), estimated with sliding–mode control (gray); b) Tracking error $\theta - \hat{\theta}$: Proposed controller (17) (black), sliding–mode control (gray).
Source: The authors.

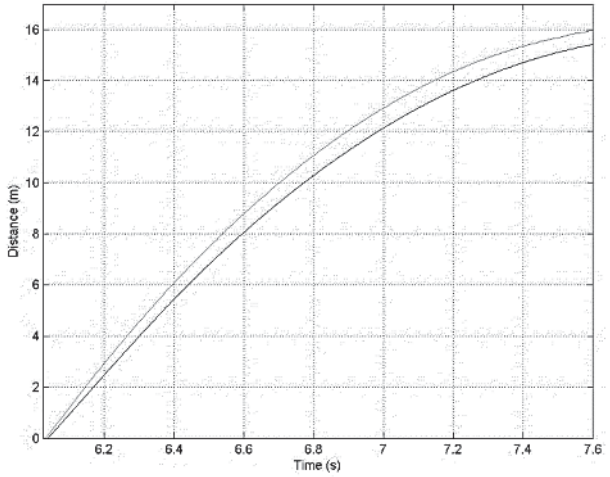

Figure 10. Braking distance: Proposed controller (17) (black), sliding-mode control (gray).
Source: The authors.

References

[1] Emig, R., Goebels, H. and Schramm, J., Antilock braking systems (ABS) for commercial vehicles-status 1990 and future prospects, Proceeding International Transportation Electronics Congress Vehicle Electronics, 1990. pp. 515-523. DOI: 10.1109/ICTE.1990.713050

[2] Kiencke, U. and Nielsen, L., Automotive control systems: For engine, driveline and vehicle, Springer. 2nd Ed, 2010.

[3] Zhen-Jun, S., Tian-Jun, Z. and Hong-Yan, Z., Research on road friction coefficient estimation algorithm based on extended Kalman filter, Proceeding of International Intelligent Computation Technology and Automation, 2008, pp. 418-422. Doi: 10.1109/ICICTA.2008.38

[4] Lin, C-H. and Chun, H., Self-learning fuzzy sliding mode control for antilock braking systems, IEEE Transaction on Control System Technology, 11(2), pp. 273-278, 2003. DOI: 10.1109/TCST.2003.809246

[5] Lennon, W.K. and Passino, K.M., Intelligent control for brake system, IEEE Transaction on Control System Technology, 7(2), pp. 188-202, 1999. DOI: 10.1109/87.748145.

[6] Wei, Z. and Xuenxun, G., An ABS control strategy for commercial vehicle, IEEE/ASME Transaction on, 20(1), pp. 384-391, 2015. DOI: 10.1109/TMECH.2014.2322629

[7] Yazdanpanah, R.M., Design of robust speed and slip controllers for a hybrid electromagnetic brake system, Electric Power Applications IET, 9(4), pp. 307-318, 2015. DOI: 10.1049/iet-epa.2014.0256.

[8] Alacalá, I., Claudio, A., Guerrero, G, Aguayo-Alquicira, J and Olivares, V.H., Electric vehicle emulation based on inertial flywheel and DC machine, DYNA 81(18), pp.86-96, 2014.

[9] Lin, W.C., Lin, C.L., Hsu, P.M. and Wu, M.T., Realization of antilock braking strategy for electric scooter, Industrial Electronics, IEEE Transaction, 61(6), pp. 2862-2833, 2014. DOI: 10.1109/TIE.2013.2276775

[10] Ivanov, V.S. and Shyrokau, B., A survey of traction control and antilock braking systems of full electric vehicle with individually controlled electric motors, Vehicular Technology, IEEE Transaction on, 64(9), pp, 3878-3898, 2015. DOI: 10.1109/TVT.2014.2361860.

[11] Inteco, User's manual, The Laboratory Antilock Braking System Controlled from PC, Inteco Ltd.Crakow, Poland, 2006.

[12] Al-Mola, M-H., Mailah, M., Samin, P.M., Muhaimin, A-H. and Abdullah, M-Y., Performance comparison between sliding mode control and active force control for a nonlinear anti-lock brake system, WSEAS Transactions on System and Control, [Online]. 9, pp. 101-107, 2014. Available at: http://www.wseas.org/multimedia/journals/control/2014/ a225703-219.pdf

[13] Martinez-Gardea, M. Mares-Guzman I.J., Di Gennaro, S. and Acosta-Lua, C., Experimental comparison of linear and non linear controllers applied to an antilock braking system, IEEE Iternational Conference on Control Applications, 2014, pp.71-76. DOI: 10.1109/CCA.2014.6981331.

[14] Precup, R.-E., Spataru, S.-V., Radac, M.-B., Petriu, E-M, Preitl, S. and David, R.-C., Experimental results of model-based fuzzy control solutions for a laboratory antilock braking system, Human Computer Systems Interaction: Backgrounds and Applications, Springer, 2012.

[15] Oniz, Y., Kayacan, E. and Kaynak, O., A Dynamic method to forecast the wheel slip for antilock braking system and its experimental evaluation, IEEE Transactions on System, Man and Cybernetics-Part B: Cybernetics, 39(2), 2009. DOI: 10.1109/TSMCB.2008.2007966.

[16] Dadashnialehi, A., Bab-Hadiashar, A., Cao, Z. and Kapoor, A., Accurate wheel speed measurement for sensorless ABS in electric vehicle, IEEE International Conference on Vehicular Electronics and Safety, 2012. pp.37-42. DOI: 10.1109/ICVES.2012.6294313.

[17] Topalov, A-V., Kayacan, E., Oniz, Y. and Kaynak, O., Neuro-fuzzy control of antilock braking system using variable structure-systems based learning algorithm, International Conference on Adaptive and Intelligent Systems, September, [Online]. 2009. pp. 166-171, Available at: http://doi.ieeecomputersociety.org/10.1109/ICAIS.2009.35

[18] Pacejka, H-B., Tyre and vehicle dynamics. Elsevier Butterworth-Hein, 2006.

[19] Kenneth, R-B., Reference input wheel slip tracking using sliding mode control, SAE Technical Paper Series, 2002-01-0301, 2002.

[20] Acosta-Lua. C., Castillo-Toledo. B., Di Gennaro. S. and Martinez-Gardea. M., Dynamic control applied to a laboratory antilock braking system, Mathematical Problems in Engineering, 2015. DOI: 10.1155/2015/896859.

[21] Utkin, V., Guldner, J. and Shi, J., Sliding mode control in electromechanical systems, The Taylor & Francis systems and control book series. Taylor & Francis, Philadelphia, PA, 1999.

C. Acosta-Lua, obtained his BSc. in Electronic Engineering from the Technological Institute of Morelia (2001), Mexico. He obtained his MSc. (2003) and PhD. (2007) in Electrical Engineering Science from CINVESTAV, Guadalajara, Mexico. He has participated in academic visits to INSA Lyon, France and DEWS Research Center in L'Aquila Italy. He undertook his Postdoctoral studies at DEWS Research Center in L' Aquila, Italy and the Ford Motor Company Centre for Research and Implementation.

Since 2009 he has been an Associate Professor of Automatic Control at the University of Guadalajara. Currently he is engaged in the development of nonlinear techniques for vehicle control and observer nonlinear subsystems.
ORCID: 0000-0002-7398-2629.

S. Di Gennaro, obtained his BSc. in Nuclear Engineering in 1987 (summa cum laude), and his PhD. in Systems Engineering in 1992, both from the University of Rome "La Sapienza", Rome, Italy. In October 1990 he joined the Department of Electrical Engineering, University of L'Aquila, as assistant professor of Automatic Control. Since 2001 he has been associate professor of Automatic Control at the University of L'Aquila. In 2012 he joined the Department of Information Engineering Computer Science and Mathematics and he is also a member of the Center of Excellence DEWS. He teaches courses in Automatic Control and Nonlinear Control. He has visited various Research Centers including the Department of Electrical Engineering of Princeton University, the Department of Electrical Engineering and Computer Science at Berkeley, and the Centro de Investigación y Estudios Avanzados del IPN in Guadalajara, Mexico. He works in the area of hybrid systems, regulation theory, and applications of nonlinear control.
ORCID: 0000-0002-2014-623X

M.E. Sanchez-Morales, obtained her BSc. in Physics in the Autonomous University of Puebla (2001), Mexico. She obtained her MSc. (2003) and PhD. (2007) in Science of Optics from CIO. She has made academic visits to CICESE Ensenada, México; UNAM México, DF; UAM Madrid, Spain and Laboratory of Physical Chemistry of Luminescent Materials in University Lyon II, Lyon France. Currently she works at the University of Guadalajara on the dynamics of movements applied to industry and optical phenomena in waveguides.
ORCID: 0000-0003-4018-672X